Biochemical Pharmacology 82 (2011) 389–399

Contents lists available at ScienceDirect

Biochemical Pharmacology

journal homepage: www.elsevier.com/locate/biochempharm

The four cysteine residues in the second extracellular loop of the human adenosine A_{2B} receptor: Role in ligand binding and receptor function

Anke C. Schiedel [a,*], Sonja Hinz [a], Dominik Thimm [a], Farag Sherbiny [b], Thomas Borrmann [a], Astrid Maaß [b], Christa E. Müller [a]

[a] PharmaCenter Bonn, Pharmaceutical Institute, Pharmaceutical Chemistry I, University of Bonn, An der Immenburg 4, D-53121 Bonn, Germany
[b] Fraunhofer Institute SCAI, Schloss Birlinghoven, 53754 Sankt Augustin, Germany

ARTICLE INFO

Article history:
Received 18 February 2011
Accepted 11 May 2011
Available online 18 May 2011

Keywords:
Adenosine A_{2B} receptor
Disulfide bonds
Extracellular loop 2
Mutagenesis
PSB-603

ABSTRACT

The adenosine A_{2B} receptor is of considerable interest as a new drug target for the treatment of asthma, inflammatory diseases, pain, and cancer. In the present study we investigated the role of the cysteine residues in the extracellular loop 2 (ECL2) of the receptor, which is particularly cysteine-rich, by a combination of mutagenesis, molecular modeling, chemical and pharmacological experiments. Pretreatment of CHO cells recombinantly expressing the human A_{2B} receptor with dithiothreitol led to a 74-fold increase in the EC_{50} value of the agonist NECA in cyclic AMP accumulation. In the $C78^{3.25}S$ and the $C171^{45.50}S$ mutant high-affinity binding of the A_{2B} antagonist radioligand [^{3}H]PSB-603 was abolished and agonists were virtually inactive in cAMP assays. This indicates that the C3.25–C45.50 disulfide bond, which is highly conserved in GPCRs, is also important for binding and function of A_{2B} receptors. In contrast, the $C166^{45.45}S$ and the $C167^{45.46}S$ mutant as well as the $C166^{45.45}S$–$C167^{45.46}S$ double mutant behaved like the wild-type receptor, while in the $C154^{45.33}S$ mutant significant, although more subtle effects on cAMP accumulation were observed – decrease (BAY60-6583) or increase (NECA) – depending on the structure of the investigated agonist. In contrast to the X-ray structure of the closely related A_{2A} receptor, which showed four disulfide bonds, the present data indicate that in the A_{2B} receptor only the C3.25–C45.50 disulfide bond is essential for ligand binding and receptor activation. Thus, the cysteine residues in the ECL2 of the A_{2B} receptor not involved in stabilization of the receptor structure may have other functions.

1. Introduction

Adenosine A_{2B} receptors belong to the large group of purinergic G protein-coupled receptors (GPCRs), which comprise P2 (P2Y and P2X, nucleotide-activated) and P1 (adenosine) receptors [1]. Brunschweiger and Müller [2] proposed to add P0 (adenine) receptors as a third class to the group of purinergic receptors. The P1 or adenosine receptor (AR) family consists of four subtypes, A_1, A_{2A}, A_{2B} and A_3 [3]. A_1 and A_3 receptors are coupled to G_i type G proteins, leading to the inhibition of the adenylate cyclase upon receptor activation, while A_{2A} and A_{2B} receptors are mainly coupled to G_s proteins resulting in an increase in intracellular cAMP concentrations via stimulation of adenylate cyclase [4]. In several cell systems, such as HEK-293 and HMC-1 mast cells A_{2B} receptors are additionally coupled to phospholipase C via G_q proteins, and are thereby linked to intracellular Ca^{2+} release [5,6]. In the human leukemia cell line Jurkat T, A_{2B}-mediated calcium mobilization independent of inositol-1,4,5-trisphosphate was observed [7]. Coupling of the A_{2B} receptor to the MAPK cascade via ERK1/2 has been described for recombinant CHO cells overexpressing human A_{2B} receptors and for mast cells, showing an involvement in proliferation, differentiation and apoptosis [4,8]. Furthermore a link of A_{2B} receptor signaling to the arachidonic acid signal transduction pathway via phospholipase A and cyclooxygenase activation leading to vasoconstriction in smooth muscle cells has been described [9].

Among the four AR subtypes A_{2B} has been the least well characterized receptor, mainly due to the lack of suitable, specific ligands [10]. Meanwhile highly selective A_{2B} antagonists have been developed and an A_{2B}-specific antagonist radioligand, [^{3}H]PSB-603 (for structure see Supplemental Figure 1), with high potency and specificity across species, including rodents and humans, has recently become available [11]. As for agonists, besides the nucleoside derivative NECA [12], which is non-selective, and related adenosine derivatives, the first highly selective A_{2B} agonist

* Corresponding author. Tel.: +49 228 736457; fax: +49 228 732567.
E-mail addresses: schiedel@uni-bonn.de (A.C. Schiedel), shinz@uni-bonn.de (S. Hinz), dthimm@uni-bonn.de (D. Thimm), fselim@uni-bonn.de (F. Sherbiny), thomas.borrmann@uni-bonn.de (T. Borrmann), astrid.maass@scai.fraunhofer.de (A. Maaß), christa.mueller@uni-bonn.de (C.E. Müller).

0006-2952/$ – see front matter © 2011 Elsevier Inc. All rights reserved.
doi:10.1016/j.bcp.2011.05.008

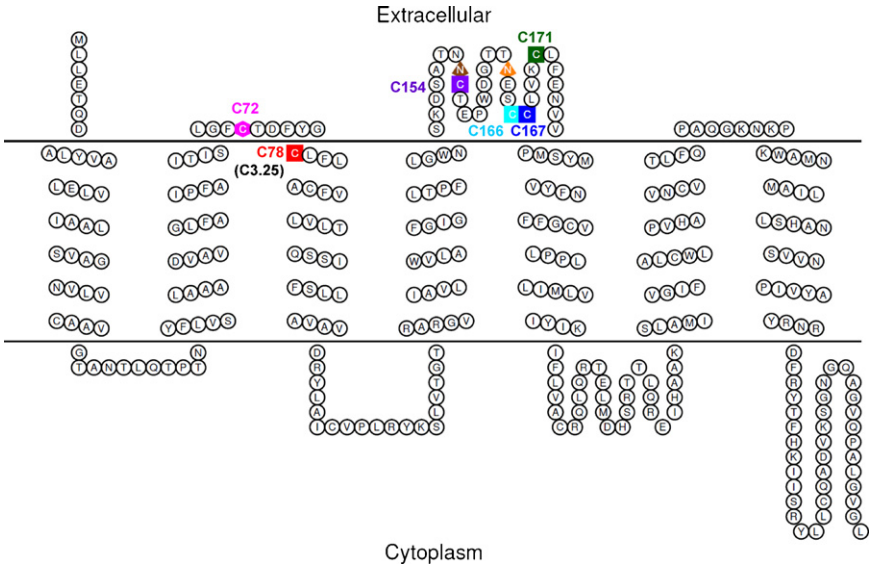

Fig. 1. Topology model of the human A_{2B} receptor. The topology of the human A_{2B} receptor is shown as a snakeplot diagram drawn with TOPO2 [36]. The amino acids are shown in the one-letter code. Cysteine residues which were exchanged for serine by site-directed mutagenesis are shown as squares and color-coded as follows: C78, red; C154, purple, C166, cyan; C167, blue; C171, green. The two potential glycosylation sites are shown as up-arrows: brown: N153; orange: N163. C72 (magenta) is shown as hexagon. (For interpretation of the references to color in this figure legend, the reader is referred to the web version of the article.)

BAY60-6583 [13], a non-nucleosidic compound, has been developed (structures are shown in Supplemental Figure 1).

In many tissues, A_{2B} receptors are considered low affinity receptors with mostly low expression levels [14]. Therefore, adenosine concentrations typically have to reach micromolar levels to activate natively expressed A_{2B} receptors, which occurs under pathological conditions, such as hypoxia, ischemia, inflammation or massive cell death [15,16]. While their distribution is ubiquitous, A_{2B} receptors are found at higher densities mainly in the large intestine, in mast cells, hematopoietic cells, and in the brain, particularly in astrocytes [6,14,17,18]. Upregulation has been found in several cancer cell lines [19]. A_{2B} receptors are thought to be involved in a number of diseases and the first antagonist is now being evaluated in clinical trials for the treatment of asthma and chronic obstructive pulmonary disease [10]. Other potential indications include secretory diarrhea associated with inflammation, Alzheimer's disease, inflammatory diseases, pain, cancer, type II diabetes, and diabetic retinopathy [20]. Thus, A_{2B} receptors represent important new drug targets.

To fully understand interactions of the human A_{2B} receptor with its ligands, agonists and antagonists, it is of major importance to gain knowledge about the structure of the receptor, the amino acid residues involved in ligand binding, and to determine the receptor's 3D structure, which in turn can then be used for the development of new ligands [21,22]. Except for a few mutagenesis studies [16,23–25] and homology models [26–28], the most recent one based on the X-ray structure of the closely related A_{2A} receptor [29], not much structural information about the A_{2B} receptor is available.

A common feature of most GPCRs is the existence of a highly conserved disulfide bond between C3.25 (Ballesteros Weinstein nomenclature [30]) at the extracellular site of transmembrane domain 3 (TMD3) and cysteine residue C45.50 [31] in the extracellular loop 2 (ECL2) located between TMD4 and TMD5 [26,27,32]. Recently de Graaf et al. [31] undertook a molecular modeling project and aligned ECL2 sequences of 365 human GPCRs. More than 92% of the investigated receptors showed the conserved disulfide bond.

The A_{2B} receptor possesses the longest ECL2 of all four adenosine receptor subtypes, with four cysteine residues – the highest number found in any GPCR – of which three (C154, C167, C171) are homologous to the three (C146, C159, C166) found in the A_{2A} receptor (see Figs. 1 and 2). Those four cysteine residues are conserved in the known mammalian A_{2B} receptor orthologs. Therefore, the goal of the present study was to investigate the role of the cysteine residues in the cysteine-rich ECL2 of the A_{2B} receptor with respect to disulfide bond formation, ligand binding, and receptor activation.

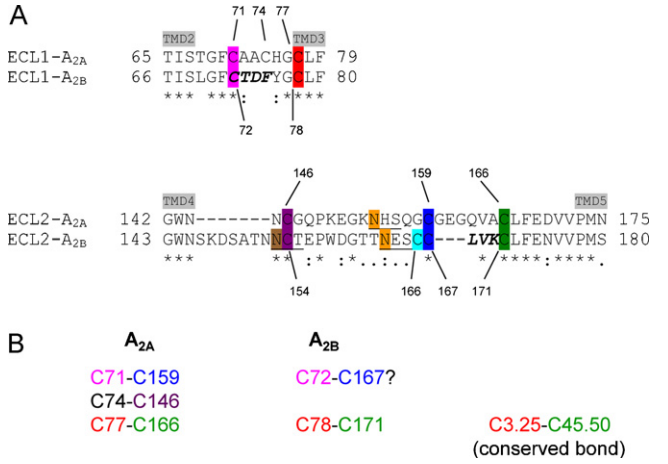

Fig. 2. (A) Alignments of the first and second extracellular loops of the human A_{2A} and A_{2B} receptors. The alignment was done using Clustal W2 [33]. The following amino acid residues are highlighted: magenta: $C71^{A2A}/C72^{A2B}$; red: conserved cysteine C3.25 in TMD3, $C77^{A2A}/C78^{A2B}$; purple: $C146^{A2A}/C154^{A2B}$; cyan: $C166^{A2A}/C166^{A2B}$; blue: $C159^{A2A}/C167^{A2B}$; green: $C166^{A2A}/C171^{A2B}$; potential N glycosylation sites: brown: $N153^{A2B}$; orange: $N161^{A2A}/N163^{A2B}$; underlined: N glycosylation seqouns; bold and italic: β-sheets; ECL: extracellular loop; (*) identical amino acid residue, (:) conserved amino acid substitution; (·) semi-conserved amino acid substitution. Amino acid positions of cysteine residues are given for the human A_{2A} and the A_{2B} receptor. (B) Cysteine residues involved in disulfide bonds found in the crystal structure of the human A_{2A} receptor [45] and cysteine residues involved in predicted disulfide bonds in the human A_{2B} receptor. (For interpretation of the references to color in this figure legend, the reader is referred to the web version of the article.)

2. Material and methods

All chemicals were obtained from Roth (Karlsruhe, Germany) or Applichem (Darmstadt, Germany) unless otherwise noted.The Radioligand [^{3}H]PSB-603 were obtained from Quotient Bioresearch (Cardiff, UK) by custom-labeling.

2.1. Alignments of extracellular loops, prediction of disulfide bonds and loop simulation

Alignments of extracellular loops 1 and 2 of the human A_{2A} and A_{2B} receptors were performed using Clustal W2 [33]. Similarity was determined using EMBOSS [34]. Prediction of N-glycosylation was done with NetNGlyc 1.0 from the CBS prediction servers [35]. The topology was illustrated using TOPO2 [36]. Modeling of the non-conserved part of the extracellular loop 2 of the adenosine A_{2B} receptor was performed with the ModLoop modeling algorithm based on global optimization of conformational energy [37]. In all models, residues in the transmembrane domains and the intracellular loops were restrained by harmonic force to their reference position during simulation; only residues of ECL1 and ECL2 were allowed to move. Loop conformations emerging from this procedure were minimized stepwise with respect to the force field energy by using the Amber package to obtain a low energy conformation [38]. Then the annealing molecular dynamics (MD) was used to optimize the accommodation of ECL1 and ECL2, where the loop atoms were heated from 100 K to 450 K and cooled to 100 K over a period of 1.6 ns. The MD simulations were performed accordingly, restraints with a force constant of 0.5 kcal/mol Å^2 were applied to TMDs for 400 ps: heated from 100 K to 450 K and 1.2 ns: then cooled from 450 K to 100 K. The time step of the simulations was 2.0 fs with a cutoff of 10 Å for the non-bonded interactions. The geometrical parameters of the created models were evaluated and compared with the crystal structure of the A_{2A} receptor using PROCHECK and PROSAII [39,40].

2.2. Cell culture

GP + envAM12 packaging cells (ATCC CRL-9641) were cultured at 37 °C and 5% CO_2 in Dulbecco's modified Eagle medium (DMEM; Invitrogen, Darmstadt, Germany), containing 10% FCS, 100 U/ml penicillin G, 100 μg/ml streptomycin, 1% ultraglutamine, 200 μg/ml hygromycin B, 15 μg/ml hypoxanthine, 250 μg/ml xanthine and 25 μg/ml mycophenolic acid. Chinese hamster ovary (CHO) cells were maintained in DMEM-F12 medium (Invitrogen, Darmstadt, Germany) with 10% FCS, 100 U/ml penicillin G, 100 μg/ml streptomycin and 1% ultraglutamine under the same conditions. All supplements were from Invitrogen (Darmstadt, Germany), and antibiotics were from Calbiochem (Merck, Darmstadt, Germany).

2.3. Site-directed mutagenesis

The coding sequence for the human adenosine A_{2B} receptor was cloned into the plasmid vector pUC19. Point mutations leading to the desired amino acid exchanges were introduced through site-directed mutagenesis using whole plasmid recombination PCR. Complementary oligonucleotide primers were designed containing the corresponding mutations. Therein, each mismatched base is flanked by 12–19 nucleotides at the 3′ and 5′ end of the primer. The PCR reaction mixture contained 20 ng of template DNA, 15 pmol of each primer, 10 mM dNTPs, 1 × Thermopol reaction buffer and 1 U $Vent_R$ polymerase (New England Biolabs, Frankfurt, Germany). The PCR was performed using the following cycle program: 4 min at 94 °C, 20 cycles consisting of 1 min at 94 °C, 1 min at 66 °C, and 10 min at 72 °C followed by a final elongation step of 10 min at 72 °C. The final PCR product was digested with the restriction enzyme *Dpn*I (New England Biolabs, Frankfurt, Germany) for 90 min to degrade any parental template DNA. After transformation of competent *Escherichia coli* Top10 cells with the digested PCR product, plasmids from single colonies were isolated and sequenced (GATC Biotech, Konstanz, Germany). Mutated receptor DNAs were subsequently subcloned into the retroviral plasmid vector pLXSN, which contained a hemagglutinin (HA) tag, resulting in an N-terminally tagged receptor after translation. Transformation, isolation and sequencing of the newly constructed plasmid were performed.

2.4. Retroviral transfection and membrane preparation

CHO cells were stably transfected using a retroviral transfection system as described before [11]. After one week the G418 concentration which is used for the selection was reduced to 200 μg/ml. For membrane preparations several dishes of stably transfected CHO cells were grown to confluence, and then cells were washed and scraped off using 50 mM Tris–HCl, pH 7.4, containing 2 mM EDTA. After homogenization the cell suspension was centrifuged for 10 min at 1000 × *g* and 4 °C. The low speed supernatant was then centrifuged at 48,000 × *g* and 4 °C for 1 h. Membrane pellets were resuspended in 50 mM Tris–HCl, pH 7.4, and centrifugation was repeated under the same conditions. Membranes were aliquoted and stored at −80 °C until further use. The protein concentration of the membrane preparation was determined using the method described by Lowry et al. [41].

2.5. Cell surface ELISA

The cell surface expression of wt and mutant receptors, stably expressed in CHO cells was determined using ELISA as previously described [42]. In brief, cells were seeded into 24 well plates 24 h before the assay. Cells were washed with PBS and blocked for 5 min with PBS/1% BSA. HA antibody (Covance, Munich, Germany) was diluted 1:1000 in DMEM, 1% BSA, 10 mM Hepes, pH 7.0, 1 mM $CaCl_2$ and added to the cells for 1 h at room temperature. After washing (3 × PBS, 5 min each) cells were fixed with 4% paraformaldehyde in PBS, washed again and blocked for 10 min. The peroxidase-coupled secondary antibody (goat anti mouse, Sigma, Munich, Germany) was diluted 1:2500 in PBS/1% BSA and added to the cells for 1 h at room temperature, after which cells were washed again 4× with PBS. 300 μl prewarmed ABTS substrate (Thermo scientific Pierce, Rockford, USA) was added and cells were incubated for 50 min. 170 μl of the substrate were transferred to 96-well plates and absorption was measured at 405 nm using fresh substrate as a reference. Experiments were performed in two to six independent experiments, each in triplicates.

2.6. Radioligand binding experiments

Competition experiments were performed using the high affinity antagonist radioligand [^{3}H]PSB-603 [11]. The wild-type receptor (wt) and the mutants C78S, C166S, C167S, and C171S were analyzed in a final volume of 500 μl. The vials contained 25 μl of the test compound dissolved in 50% DMSO/50% Tris–HCl (50 mM, pH 7.4), 275 μl of 50 mM Tris–HCl buffer (pH 7.4), 100 μl of radioligand solution in the same buffer (final concentration 0.3 nM), and 30 μg of membrane preparations (diluted in 100 μl Tris–HCl, pH 7.4) which had been preincubated with adenosine deaminase (ADA, 2 U/ml) for 20 min. The mutants C154S and C166S–C167S were analyzed in radioligand binding assays in a final volume of 200 μl containing 50 μl of test compound diluted in 10% DMSO/90% Tris–HCl (50 mM, pH 7.4), 50 μl radioligand diluted in Tris–HCl buffer (50 mM, pH 7.4, final concentration of

the radioligand 0.3 nM) and 50 μg of membrane preparations, diluted in 100 μl buffer, pretreated with ADA (2 U/ml) 20 min before use. Total binding was determined in the absence of test compound; nonspecific binding was measured in the presence of 10 μM 8-cyclopentyl-1,3-dipropylxanthine (DPCPX). After 75 min at room temperature samples were harvested by filtration through GF/B glass fiber filters. Filters were washed with ice-cold buffer containing 50 mM Tris–HCl (pH 7.4) and 0.1% bovine serum albumin (BSA), and subsequently transferred into scintillation vials. The liquid scintillation counting of the filters started after 9 h of pre-incubation in 2.5 ml of scintillation cocktail (Lumag AG, Basel) in order to allow the radioligand to diffuse into the scintillation cocktail. Three independent experiments were performed each in triplicates. If the sample volume for incubation was reduced to 200 μl depletion occurred due to the high affinity and low concentration of the radioligand [^{3}H]PSB-603, which means that the free ligand concentration in the solution was actually lower than the concentration added [43].

2.7. Saturation assays

Saturation experiments were performed in duplicates as described in paragraph 2.6 with radioligand concentrations ranging from 0.05 to 1.6 nM in 50 mM Tris–HCl (pH 7.4).

2.8. Determination of intracellular cAMP accumulation

Stably transfected CHO cells expressing the wild-type or mutant receptors were plated onto 24 well plates at a density of 200,000 cells per well. After 24 h the medium was removed and the cells were washed with 500 μl of 37 °C warm Hank's Balanced Salt Solution (HBSS; 20 mM HEPES, 135 mM NaCl, 5.5 mM glucose, 5.4 mM KCl, 4.2 mM $NaHCO_3$, 1.25 mM $CaCl_2$, 1 mM $MgCl_2$, 0.8 mM $MgSO_4$, 0.44 mM KH_2PO_4 and 0.34 mM Na_2HPO_4, pH adjusted to 7.3) containing 1 U/ml of adenosine deaminase (ADA, Sigma). The cells were then incubated in 300 μl of HBSS with ADA at 37 °C and 5% CO_2 for 2 h. Then, 100 μl of the phosphodiesterase inhibitor Ro20-1724 (Hoffmann La Roche, Grenzach, Germany; final concentration 40 μM) were added to each well and the cells were incubated for 15 min at 37 °C and 5% CO_2. Then 100 μl of various dilutions of the agonists 5′-N-ethylcarboxamidoadenosine (NECA; Sigma, Munich, Germany), or BAY60-6583 (Bayer Schering Pharma), respectively in HBSS containing 5% DMSO were added in triplicates (final DMSO concentration 0.5%). After 15 min of incubation at 37 °C and 5% CO_2 the supernatant was removed and 500 μl of 90 °C hot lysis buffer consisting of 4 mM EDTA and 0.01% Triton X-100 with the pH adjusted to 7.3 were added. After one hour of mixing on ice, cAMP amounts of the lysates were determined by competitive radioligand binding experiments [44]. Competition experiments were performed in a final volume of 120 μl containing 50 μl of cell lysates, 30 μl of [^{3}H]cAMP radioligand solution in lysis buffer (final concentration 3 nM) and 40 μl of cAMP binding protein [44] diluted in the same buffer (50 μg per sample). For determining cAMP concentrations 50 μl of various cAMP concentrations were measured instead of cell lysates, to obtain a standard curve. Total binding was determined by adding radioligand and binding protein to lysis buffer, and the background was determined without addition of binding protein. The mixture was incubated for 60 min on ice and filtered through a GF/B glass fiber filter using a cell harvester (Brandel, Unterföhring, Germany). The filters were washed three times with 2–3 ml of ice-cold 50 mM Tris–HCl buffer, pH 7.4 and subsequently transferred into scintillation vials. The liquid scintillation counting of the filters started after 9 h of incubation in 2.5 ml of scintillation cocktail (Lumag AG, Basel). Three separate experiments were performed. The amount of cAMP was determined by comparison to a standard curve generated for each experiment and plotted as percent of maximal NECA stimulation.

2.9. Experiments with DTT pretreatment

The effect of dithiothreitol (DTT) on receptor function was investigated by measuring NECA-induced cAMP accumulation as described in 2.8, except that CHO cells, stably expressing the human A_{2B} receptor, were preincubated with 10 mM DTT for 2 h at 37 °C.

3. Results

3.1. Comparison of extracellular loops 1 and 2 of A_{2A} and A_{2B} receptors

The A_{2A} receptor is the adenosine receptor subtype, which is most closely related to the A_{2B} receptor. Sequence analysis of the human A_{2A} and A_{2B} receptors show an overall identity of 58% and a similarity of 73%. The most conserved residues are found within the transmembrane domains. By comparing the extracellular loops 1 and 2, which show 44% and 34% identity, and 56% and 46% similarity, respectively, one can find extremely high degrees of homology when comparing the residues close to the cysteine residues C71, C77, C166 in the A_{2A} receptor and the corresponding residues C72, C78, C171 in the A_{2B} receptor (see Fig. 2). The residues adjacent to those cysteine residues are identical or at least similar in A_{2A} and A_{2B} receptors in both extracellular loops. The region between the conserved cysteine C45.50 (C166 in A_{2A}, C171 in A_{2B}) in ECL2 and TMD5 is even 86% identical and 100% similar, providing evolutionary evidence for the importance of that partial structure. The ECL2 of both receptors contain potential N-glycosylation sites between the highly similar stretch between the conserved cysteine residues C146 and C159 in the A_{2A} receptor, and C154 and C167 in the A_{2B} receptor, respectively. The A_{2B} receptor contains a second potential N-glycosylation site at N153, where C154 is part of the sequon. The A_{2B} receptor has a 7-amino acid insertion at the site close to TMD4 and a 3-amino acid gap between the conserved cysteine residues C167 and C171, moving those cysteine residues and the adjacent glycosylation site closer together as compared to the A_{2A} receptor. The crystal structure of the A_{2A} receptor [45] shows two β-sheets in ECL1 and ECL2 both being in an antiparallel conformation. According to the refined computer model based on the published model [29], the A_{2B} receptor can also form one β-sheet in each of the extracellular loops 1 and 2, which appear to be close enough together to be able to form antiparallel sheets. Despite similarities between the adenosine A_{2A} and the A_{2B} receptor subtypes with regard to the cysteine residues localized close to or in the extracellular part of the proteins there are significant differences, and their roles and functions may be different.

3.2. Disulfide bond prediction

For predicting disulfide bonds in the ECL2 of the A_{2B} receptor, models of the A_{2A} receptor based on the published X-ray structure were initially generated for testing the procedure. One of the generated models (m1 A_{2A}) contained the highly conserved disulfide bond between C3.25 and C45.50, corresponding to C77 (TMD3) and C166 (ECL2), while a second model (m2 A_{2A}) contained all four possible bonds (C77–C166, C74–C146, C71–C159, and C259–C262), which were observed in the X-ray structure of the A_{2A} receptor [45]. Table 1 lists the fixed disulfide bonds and the results of the analyses used to evaluate the goodness of the models obtained by several programs, such as PROCHECK (psi/phi angles), PROSAII (Z-scores) and root mean square distances (RMSD), both in comparison to the A_{2A} X-ray structure and the initial A_{2A} or A_{2B}

Table 1
Evaluation of the goodness of different A_{2A} and A_{2B} receptor models after simulation.

	m1 A_{2A}	m2 A_{2A}	m1 A_{2B}	m2 A_{2B}	m3 A_{2B}	m4 A_{2B}
Disulfide bonds fixed before simulation	C77–C166	C71–C159 C74–C146 C77–C166 C259–C262	C78–C171	C72–C167 C78–C171	C72–C166 C78–C171	C72–C167 C78–C171 C154–C166
PROCHECK psi/phi angels[a]	1.1	0.4	0.7	0.7	0.7	1.0
PROSAII *Z*-score[b]	−4.3	−4.11	−4.06	−3.91	−4.17	−4.42
RMSD[c] relative to the A_{2A} crystal structure (Å)	1.0	0.8	1.3	1.9	1.7	1.7
RMSD relative to initial structure (Å)	0.9	0.8	0.7	1.0	0.8	0.8

[a] psi (angle between carbon and carbonyl) and phi angels (angle between carbon and nitrogen) are determined using a Ramachandran plot, which is a way to visualize the dihedral angles (psi against phi) of amino acid residues in protein structures. Lower values indicate better quality.
[b] The *Z*-score indicates the overall model quality, its value is displayed in a plot which shows the local model quality by plotting energies as a function of the amino acid sequence position. In general, positive values correspond to problematic parts of the input structure, negative values indicate good quality.
[c] RMSD: root mean square distance. Lower overall values indicate good accordance between two models.

model. The psi/phi angles, which are obtained by PROCHECK are determined using a Ramachandran plot, which is a way to visualize the dihedral angles (psi against phi) of amino acid residues in protein structures, where psi is the angle between carbon and carbonyl and phi the angle between carbon and nitrogen. Lower values indicate better quality of the model. *Z*-scores, obtained by PROSAII, indicate the overall model quality; its value is displayed in a plot which shows the local model quality by plotting energies as a function of the amino acid sequence position. In general, positive values correspond to problematic parts of the input structure, negative values indicate good quality. RMSD values are a useful way to compare two models either of the same structure or two closely related structures, such as the crystal structure of the A_{2A} receptor and the model of the A_{2B} receptor. The values reflect the average distances between the backbones of the proteins. Lower values indicate good accordance between two models or structures. Model 2, containing all four disulfide bonds, observed in the A_{2A} crystal structure (m2 A_{2A}) led to better values and scores and was therefore chosen as reference for the predictions of disulfide bonds in the A_{2B} receptor (see Table 1). Four different A_{2B} receptor models with combinations of fixed disulfide bonds were compared to m2 A_{2A} and the initial A_{2B} model without any disulfide bonds [29]. Fig. 3A shows the positions of the cysteine residues potentially involved in disulfide bond formation in the initial A_{2B} model before loop simulation, as well as the two asparagine residues, which could be glycosylated. According to the Z-score, model 2 (m2 A_{2B}) containing two disulfide bonds, C78–C171 and C72–C167, would be the preferred model, since positive values correspond to problematic parts of the input structure while negative values indicate high quality. According to all other parameters determined, model 1 (m1 A_{2B}), containing only the highly conserved disulfide bond between TMD3 and ECL2, C78–C171, is the most likely prediction. The more significant analysis of the loop motions during simulation allows a comparison of the fluctuation profiles along the sequences of all models (see Fig. 4). Since all protein parts except for ECL1 and ECL2 have been restrained to their initial position during simulation, only motions in the ECL1 and ECL2 segments are observed. It was found that m1 A_{2B} and m4 A_{2B}, i.e. the model with the lowest number of disulfide bonds and the one with the highest number of disulfide bonds, produce B-factor profiles very similar to the one of the tightly constrained m2 A_{2A} model with four disulfide bonds. B-factors indicate the true static or dynamic mobility of an atom; it can also indicate errors in model building (reflected in higher values, corresponding to the peaks in Fig. 4). However, introducing a disulfide bond between C72–C166 and C72–C167, respectively, apparently leads to a structural destabilization. The analysis of average B-factors shows a preference for models 1 and 4 (see Fig. 4). ECL2 contains two potential glycosylation sites, N153 and N163, both close to cysteine residues. In model 1 and model 2 both sites are accessible for glycosylation. As shown in Fig. 3B, in model 1 the two extracellular loops 1 and 2 are held together by two antiparallel β-sheets, while the loops in model 2 are connected by a second disulfide bond between C72 and C167. The β-sheet in

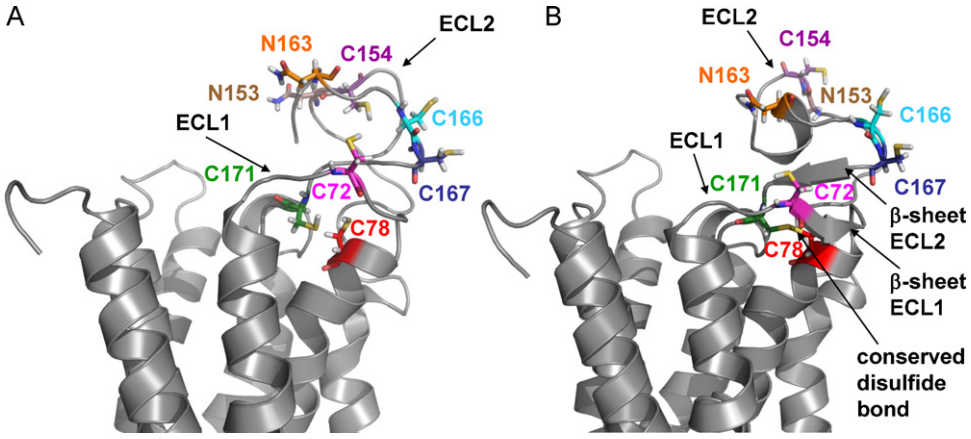

Fig. 3. Molecular models of the human adenosine A_{2B} receptor. (A) Initial model without fixed disulfide bonds (starting conformation). (B) Model 1 A_{2B} after simulation with one fixed disulfide bond: C78–C171 (m1 A_{2B}). The following amino acids are shown as stick models: magenta: C72; red: C78; purple: C154; cyan: C166; blue: C167; green: C171; potential N glycosylation sites: brown: N153 and orange: N163. (For interpretation of the references to color in this figure legend, the reader is referred to the web version of the article.)

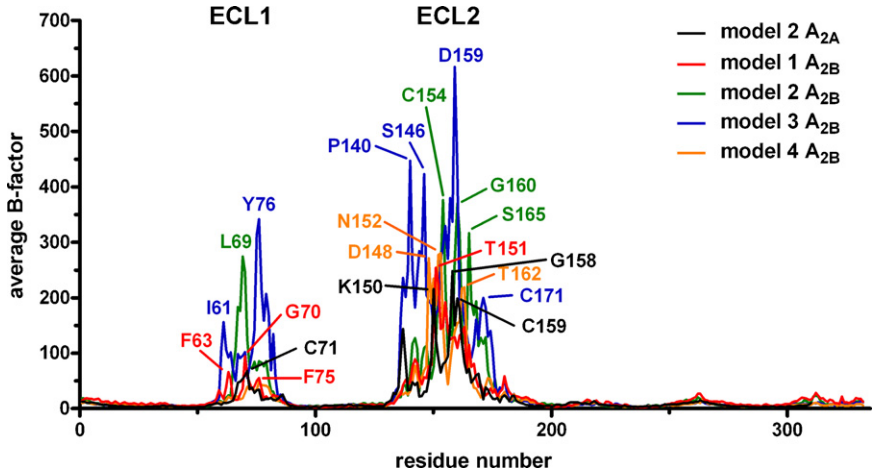

Fig. 4. Comparison of B-factors for the disulfide bond predictions of the four simulated models of the human A_{2B} receptor and for model 2 of the human A_{2A} receptor. B-factors indicate the true static or dynamic mobility of an atom, it can also indicate where there are errors in model building. Higher values indicate higher mobility of residues.

ECL1 appears to be very stable, while the β-sheet in ECL2 was less stable during the simulation process. With the β-sheet present in ECL2, C72 and C167 are about 10 Å apart, making it very unlikely to form a disulfide bond. Model 3, having a second disulfide bond between C72 and C166, is less likely than models 1 and 2 according to the values and scores (see Table 1), and model 4 can be excluded because of unfavorable values (see Table 1), in addition, both potential glycosylation sites are not exposed to the solvent, but are facing the helices. Thus, molecular modeling studies indicate that the A_{2B} receptor might contain a second disulfide bond (C72–C167) next to the highly conserved bond between C78 and C171 (model 2).

3.3. Effects of DTT pretreatment on A_{2B} receptor activity

A first experimental indication that disulfide bond formation is essential for A_{2B} receptor function was obtained by preincubating CHO cells stably expressing human A_{2B} receptors with DTT followed by NECA-induced cAMP accumulation assays. As shown in Fig. 5 the curve for the agonist NECA was shifted to the right by 74-fold compared to A_{2B} receptor activity without DTT pretreatment (EC_{50} values: 2720 nM vs. 36.6 nM).

3.4. Comparison of A_{2B} wild-type receptors with and without HA tag

As a next step we planned to exchange each of the cysteine residues in ECL2 of the human A_{2B} receptor for serine. For comparison of the mutant receptors with the wild-type receptor it was essential to determine their cell surface expression by ELISA. Therefore tagging of the receptors was required. Receptors were HA-tagged at the N terminus, which had been shown not to interfere with ligand binding and function for several other GPCRs [42]. Potential interference of the tag at the A_{2B}AR was investigated in radioligand binding as well as in functional assays. As shown in Fig. 6 binding of ligands to the HA-tagged A_{2B} receptor was not altered in comparison to the wt receptor. K_D values (untagged wt: 0.403 ± 0.188 nM, HA-tagged wt: 0.473 ± 0.170 nM) calculated from saturation experiments were not significantly different (see Fig. 7). Although B_{max} values (untagged wt: 502 ± 57 fmol/mg, HA-tagged wt: 283 ± 37 fmol/mg) differed slightly, expression of both, tagged and untagged receptors was in the same range. Neither for the antagonist PSB-603 nor for the agonists NECA and BAY60-6583 significant differences of K_i values determined in radioligand binding studies could be found (see Supplemental Table 1 and Fig. 6). When comparing the functionality of the HA-tagged receptors to the wild-type receptors no significant differences could be detected either. Fig. 8 shows the results of cAMP accumulation experiments using whole cells with two structurally different agonists, NECA (Fig. 8A) and BAY60-6583 (Fig. 8B and Supplemental Table 1). For NECA, EC_{50} values of 26.9 ± 4.5 nM (untagged) and 36.6 ± 4.8 nM (tagged) were determined, and for BAY60-6583 37.5 ± 12.3 nM and 42.4 ± 4.4 nM, respectively.

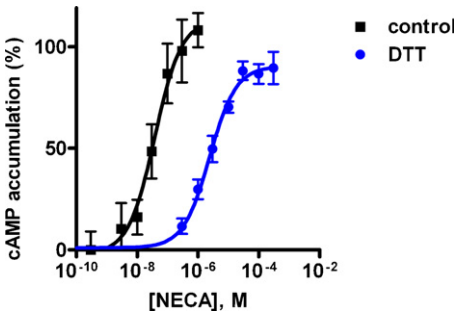

Fig. 5. Effect of preincubation with DTT on A_{2B} receptor activity. NECA-induced cAMP accumulation in CHO cells stably expressing the human A_{2B} receptor without and with DTT pretreatment (10 mM DTT, 2 h at 37 °C). Data points represent mean values ± SEM from three independent experiments performed in triplicates. Determined EC_{50} values: control: 36.6 ± 4.8 nM, DTT-pretreated: 2720 ± 570 nM.

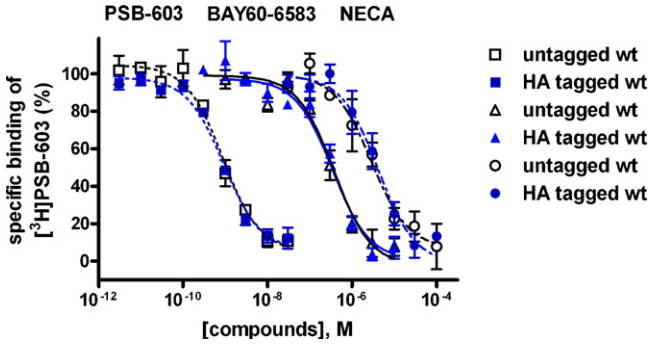

Fig. 6. Competition binding experiments of standard ligands at HA-tagged and untagged human adenosine A_{2B} receptors. Radioligand binding experiments were performed at membrane preparations of CHO cells stably expressing the human A_{2B} receptor using the antagonist [^{3}H]PSB-603 (0.3 nM) as a radioligand. Data points represent means ± SEM of three independent experiments performed in triplicates. IC_{50} and K_i values are listed in Supplemental Table 1. Results from untagged and HA-tagged receptors were not significantly different.

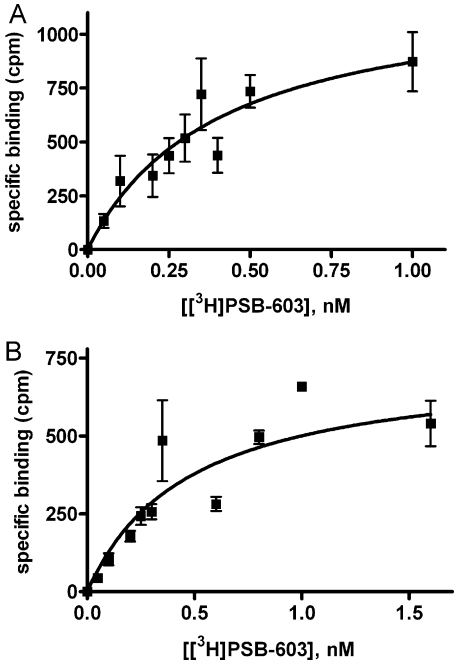

Fig. 7. Saturation binding of [^{3}H]PSB-603 to human adenosine A_{2B} receptors (A) without and (B) with HA tag, stably expressed in CHO cells. Data points represent means ± SEM of three independent experiments performed in duplicates. K_D value for untagged A_{2B} receptors: 0.403 ± 0.188 nM, for HA-tagged A_{2B} receptors: 0.473 ± 0.170 nM (not significantly different). Determined B_{max} values were 502 ± 57 fmol/mg protein (A), and 283 ± 37 fmol/mg protein (B).

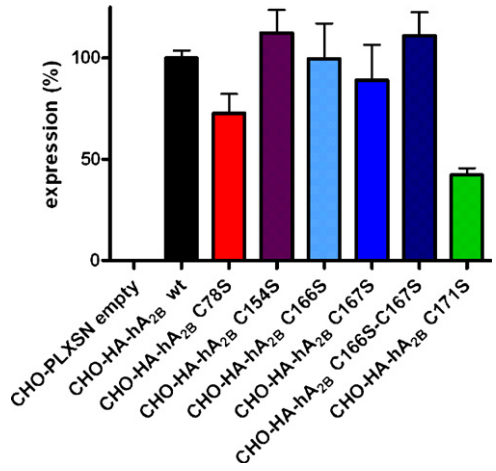

Fig. 9. Cell surface expression levels of mutant receptors in comparison to the wt A_{2B} receptor determined by ELISA. Values were normalized versus values from cells transfected with the empty plasmid, set at 0% and values from cells expressing the wt receptor, set at 100%. Data represent the mean values ± SEM of two (C166S–C167S, C171S), three (empty, C78S, C154S, C166S, C167S), or six (wt) independent experiments performed in triplicates.

3.5. Characterization of mutant receptors

All receptor cDNA sequences were subcloned into the retroviral expression vector pLXSN and stably expressing CHO cells were generated. Cysteine residues (C78, C154, C166, C167, and C171) which were replaced by serine via site directed mutagenesis are highlighted in a topology model of the A_{2B} receptor (Fig. 1). Cell surface expression levels for all mutants were determined by ELISA and compared to that of the wt receptor (see Fig. 9)

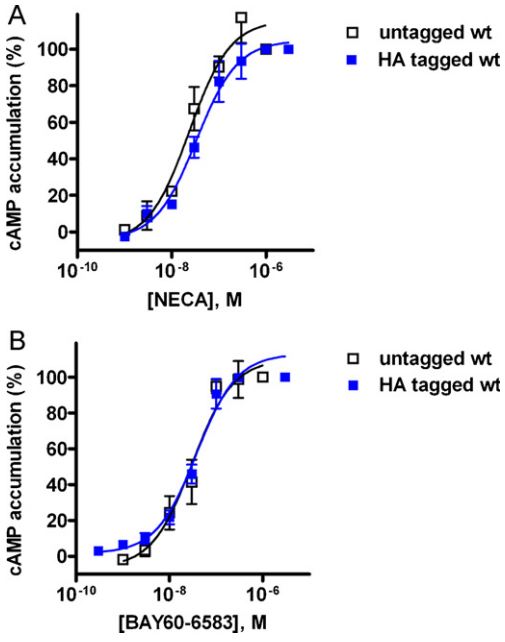

Fig. 8. Agonist induced cAMP accumulation in CHO cells stably expressing HA-tagged or untagged A_{2B} receptors using (A) NECA, or (B) BAY60-6583 as agonists. Data points represent mean values ± SEM from three independent experiments performed in duplicates. Corresponding EC_{50} values are summarized in Supplemental Table 1. Results from untagged and HA-tagged receptors were not significantly different.

Cysteine mutants were analyzed in radioligand binding studies using the antagonist radioligand [^{3}H]PSB-603 versus unlabeled PSB-603 as well as versus the agonist NECA (see Supplemental Figure 2). All mutants were compared to the wt receptor. Binding of [^{3}H]PSB-603 (0.3 nM) to C78S and C171S mutants was completely abolished; therefore no competition binding curves could be determined. In contrast, the mutants C166S, C167S, and the double mutant C166S–C167S showed similar affinity for PSB-603 and NECA as the wt receptor. A difference was, however, seen with C154S: it exhibited a significantly, 8-fold increased IC_{50} value for PSB-603, while no significant difference was observed for the agonist NECA (Table 2).

NECA-induced cAMP accumulation was examined using cells expressing the generated mutants (Fig. 10A). In contrast to the mutants C166S, C167S, and C166S–C167S, which showed EC_{50} values that were not significantly different from that determined at the wt, the mutants C78S, C154S, and C171S showed significantly increased EC_{50} values compared to the wild-type receptor (Table 3). While the EC_{50} value for the mutant C154S was moderately (2.7-fold) increased, the dose–response curves for the mutants C78S and C171S were dramatically shifted to the right, resulting in

Table 2
Affinities of the antagonist PSB-603 and the agonist NECA at the human A_{2B} receptor mutants and the wt receptor determined in radioligand binding studies versus [^{3}H]PSB-603 (0.3 nM). Data are means ± SEM of three independent experiments unless otherwise noted.

wt or mutant	PSB-603 IC_{50} ± SEM (nM)	NECA IC_{50} ± SEM (nM)
wt	2.39 ± 0.71[a]	5300 ± 946[b]
C78S	–[c]	–[c]
C154S	19.0 ± 4.3[***]	4970 ± 490[ns]
C166S	1.41 ± 0.15[ns]	4253 ± 766[ns]
C167S	1.60 ± 0.38[ns]	2933 ± 121[ns]
C166S–C167S	5.49 ± 1.30[d,ns]	3920 ± 517[ns]
C171S	–[c]	–[c]

Results of two-tailed *t*-test: [ns]not significantly different from wild type, [***]$p < 0.001$.
[a] $n = 6$.
[b] $n = 5$.
[c] Could not be determined since [^{3}H]PSB-603 did not show high affinity binding to the mutants.
[d] $n = 2$.

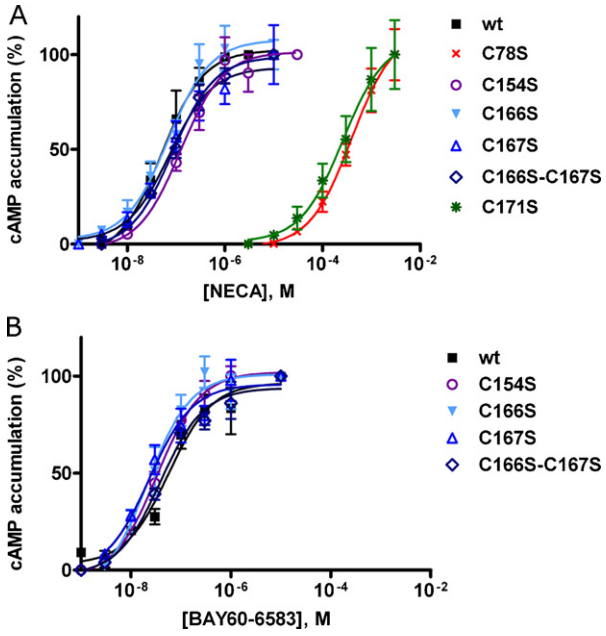

Fig. 10. Agonist-induced cAMP accumulation studies in CHO cells stably expressing the wt and cysteine mutants of the human A_{2B} receptor using (A) NECA, and (B) BAY60-6583 as agonists. Data represent mean curves ± SEM from six (wt) or three (mutants) independent experiments performed in duplicates. Corresponding EC_{50} values are summarized in Table 3. The C78S and C171S mutants could not be activated by BAY60-6583 at concentrations which were soluble (solubility < 30 μM).

an almost 7000-fold increase in the EC_{50} value in the mutant C78S (397,000 ± 7700 nM) compared to that of the wild-type receptor (58.1 ± 1.2 nM), and a similarly large increase for the mutant C171S (to 256,000 ± 28,900 nM). At the mutated receptors C78S and C171S the EC_{50} of the non-nucleosidic agonist BAY60-6583 was also dramatically increased, similarly as observed for NECA. Due to the limited solubility of BAY60-6583 full concentration-response curves could, however, not be determined. In the other cysteine mutants C154S, C166S, and C167S BAY60-6583 showed slightly decreased EC_{50} values (only ca. 2-fold; see Fig. 10B and Table 3).

4. Discussion

The extracellular loops ECL1 [25], ECL2 [31], and ECL3 [42] of GPCRs belonging to the rhodopsin family have been found to contribute considerably to receptor function [46]. However, extracellular loops differ widely in length, sequence, and structure between different GPCRs and even between closely related receptor subtypes [31]. Cysteine residues and disulfide bonds present in the extracellular domains of GPCRs have been reported to play important roles in ligand binding, receptor stability, and receptor function [32,47,48]. The adenosine A_{2B} receptor contains the highest number of cysteine residues in the ECL2 of all mammalian GPCRs (C154, C166, C167, C171) [31]. Therefore we were interested in studying the role of these cysteine residues and their potential involvement in the formation of disulfide bonds.

Most rhodopsin-like GPCRs contain a disulfide bond between the highly conserved cysteine residue C3.25 corresponding to C78 in the A_{2B} receptor, which is located in TMD3 and the conserved cysteine residue C45.50 in the second extracellular loop (C171 in A_{2B}). For several GPCRs this disulfide bond has been shown to play a critical role for correct receptor conformation and activation [47]. The ECL2 is especially known to be involved in antagonist binding, which could experimentally be shown for several receptors, e.g. the dopamine D2 receptor [49] and the adenosine A_3 receptor [50]. Compared to the ECL2 of the other adenosine receptor subtypes, the ECL2 of the A_{2B} receptor shows several differences: (i) the loop is between 4 and 10 amino acids longer; (ii) ECL2 contains the most cysteine residues, four compared to three in A_{2A}, all of which are involved in disulfide bonds according to the A_{2A} receptor crystal structure [45], and only one in A_1 and A_3 receptors; (iii) the loop has two potential N-glycosylation sites compared to only one in each of the other adenosine receptor subtypes. The highest conservation of the ECL2 is found in the part of ECL2 which is close to TMD5. The sequence upstream of the conserved cysteine is shorter than the corresponding sequence in bovine rhodopsin, 9 amino acids compared to 14 amino acids [31]. The conserved area between C45.50 and TMD5 is also very close to the binding pocket and stabilized by the essential disulfide bond between TMD3 and ECL2, and therefore probably not very flexible, while the less conserved area closer to TMD4 is highly flexible and might be involved in ligand selection, or function as a cap in analogy to the gated entrance pores described for several GPCRs [31,51]. The β-sheet just upstream of the conserved disulfide bond further stabilizes this end of ECL2. In the X-ray structure of the A_{2A} receptor a second disulfide bond is holding the β-sheet in place making this area even less flexible. This part of the loop could therefore be at least partly responsible for the high affinity of the A_{2A} receptor for adenosine and related agonists by stabilizing the active conformation. The loop in the A_{2A} receptor is shorter, and thus, the entrance to the binding pocket is probably open and more accessible to the ligands. This hypothesis may also explain why A_{2B} receptors typically show lower affinity for adenosine and adenosine derivatives (agonists) than A_{2A} receptors, since the longer ECL2 of the A_{2B} receptors may in some cases partially block the entrance to the binding pocket. The ECL2 might be involved in transient, low-affinity ligand binding. Especially binding of large ligands with long substituents extending to the receptor surface may interfere with ECL2 movement or "gate closing". This might explain the effect of the C154S mutant on PSB-603 binding. ECL2 movement may also be required for proper receptor activation. In accordance with this hypothesis is the finding of Bokoch et al.

Table 3
EC_{50} values determined for the agonists NECA and BAY60-6583 in cAMP accumulation assays at the wt and the mutants of the human A_{2B} receptor. Data are means ± SEM of three independent experiments unless otherwise noted.

wt or mutant	NECA EC_{50} ± SEM (nM)	Fold shift[a]	BAY60-6583 EC_{50} ± SEM (nM)	Fold shift[a]
wt	58.1 ± 11.7[b]		62.8 ± 7.3[c]	
C78S	397 000 ± 7700***	6830	>100,000***	>1590
C154S	159 ± 29**	2.7	35.9*	0.6
C166S	71.1 ± 12.6^{ns}	1.2	26.8 ± 6.1*	0.4
C167S	64.5 ± 6.5^{ns}	1.1	26.3 ± 5.5*	0.4
C166S–C167S	94.1 ± 13.0^{ns}	1.6	40.6^{ns}	0.6
C171S	256,000 ± 28,900***	4400	>100,000***	>1590

Results of a two-tailed *t*-test: ^{ns}not significantly different from wild type, $^{*}p < 0.05$, $^{**}p < 0.01$, $^{***}p < 0.001$.
[a] The shift represents the ratio EC_{50} (mutant): EC_{50} (wt).
[b] $n = 6$.
[c] $n = 5$.

describing ligand-induced conformational changes of the extracellular surface of the β2 adrenergic receptor (β_2AR), especially involving ECL2 and ECL3 [51]. They also describe the formation of a structured cap which covers the opening of the binding pocket once a ligand is bound, involving ECL2 and a salt bridge between an aspartate residue and a lysine residue connecting ECL2 and ECL3. The A_{2B} receptor exhibits those amino acids in equivalent positions (K269 at the transition from ECL3 to TMD7 corresponding to Lys305 in the β_2AR and Asp159 in ECL2 corresponding to Asp192 in the β_2AR, rendering a similar mechanism probable [51].

Dithiothreitol, a disulfide-reducing agent, which is commonly used to investigate the importance of disulfide bonds in proteins, was applied to examine whether the A_{2B} receptor possesses essential disulfide bonds necessary for receptor function [42]. As shown in Fig. 5 a dramatic decrease in receptor function could be observed which has also been shown for some other GPCRs containing the conserved disulfide bond connecting TMD3 and ECL2 [42,45]. These results clearly show that at least one disulfide bond, susceptible to DTT reduction and, thus, presumably exposed to the surface of the cell membrane, is important for receptor function.

Subsequently each cysteine residue of the A_{2B} receptor located in the ECL2, as well as C78 in the external half of TMD3 was individually replaced by the sterically and electronically similar serine, which lacks the ability to participate in disulfide bond formation but is still able to form H-bonds, which are even stronger for the OH group of serine than for the original SH group of its cysteine homologue. Through site-directed mutagenesis DNA constructs coding for the mutations C78S (TMD3), C154S, C166S, C167S, and C171S (ECL2) of the A_{2B} receptor were generated. In addition, a C166S–C167S double mutant was constructed. To obtain comparable EC_{50} values mutants were compared to cells overexpressing wild-type receptors at the same level. Therefore shifts of EC_{50} values were due to reduced binding or function and not due to different expression levels. Only two mutants, C78S and C171S showed somewhat lower expression levels.

As predicted by the A_{2B} model it could clearly be shown, that C78 in TMD3 and C171 in ECL2 are forming an important disulfide bond. The results obtained in radioligand binding as well as functional studies showed a dramatic decrease in IC_{50} and EC_{50} values of several thousand-fold for the mutants C78S and C171S. All other mutants either showed no difference or only moderate changes compared to the wild-type receptor. It is known that disulfide bonds are already formed in the endoplasmic reticulum (ER) and are very often necessary for proper folding and transport to the Golgi apparatus. Therefore mutants without essential disulfide bonds are more prone to degradation than wild-type receptors, further explaining somewhat lower cell surface expression levels [47,52]. While EC_{50} values determined in functional studies may be dependent on the receptor expression level, affinities measured in radioligand binding studies are not. The extreme rightward shift of the concentration response curves in functional assays can also not be explained by the somewhat lower expression levels in the mutant receptors, which would be expected to cause only a moderate shift at the most [42]. Thus it can be concluded that the disulfide bond C78–C171 in A_{2B} receptors is essential for ligand binding and receptor function.

Based on the results of radioligand binding and functional assays as well as loop simulations (Figs. 4, Supplemental Figure 2, 10; Tables 1–3), model m1 A_{2B}, containing only the conserved disulfide bond between C78 and C171, represents the most likely structure. It was shown that this disulfide bond is essential for proper receptor function (Fig. 10). According to our experimental data, all other disulfide bonds that had been predicted or might be formed are less likely. If C72, located in the first extracellular loop, was involved in linking ECL1 and ECL2 via a disulfide bond, similar to the situation found in the A_{2A} X-ray structure [45], and this bond was essential for receptor function, one of the ECL2 cysteine mutants should show different properties than the wild-type receptor. ECL1 and ECL2 are held together by antiparallel β-sheets as predicted by the model m1 A_{2B}. Both β-sheets are also present in the A_{2A} receptor [45]. Two of the possible cysteine residues proposed to be involved in forming a hypothetical second disulfide bond with C72, namely C166 and C167 (m2 A_{2B} and m3 A_{2B}), are located adjacent to the putative N-glycosylation site N163. Disulfide bond formation usually prevents glycosylation of nearby glycosylation sites. When a disulfide bond cannot be formed due to mutagenesis of cysteine residues, substitution of normally unused glycosylation sites is common [53]. In case C166 or C167 would be involved in a second disulfide bond with C72, N163 could be glycosylated in the cysteine mutants C166S, C167S, and C166S–C167S. This glycosylation might then change the conformation of the receptor leading to larger amounts of misfolded protein and to more degradation and, as a consequence, to lower levels of cell surface expression, which was, however, not observed in our mutants (see Fig. 9). Alternatively, N163-glycosylation could result in changes in ligand binding and/or to altered function of the mutant receptors. However, in both mutants, C166S and C167S as well as in the double mutant C166S–C167S neither changes in expression nor binding and receptor function could be observed. This leads to the conclusion that both, disulfide bond formation as well as glycosylation is unlikely. A further candidate cysteine residue potentially involved in forming a hypothetical second bond with C72 is C154. This amino acid residue is the central part of the sequon N-X-S/T for the putative N-glycosylation site N153. If the bond were essential, an effect of the C154S in ligand binding and receptor function were to be expected. If the bond is not formed, glycosylation of N153 would be likely and should not be affected by the cysteine to serine exchange, since the sequon N-X-S/T allows any amino acid except for proline in the middle position. Thus, no change in ligand binding and receptor function should be expected in the mutant if no disulfide bond is formed. Interestingly, A_{2B} receptors from birds and bony fish, which only possess two cysteine residues in the ECL2 show the closely related serine residue at that position. From the evolutionary point of view they have developed independently from the mammalian A_{2B} receptors because they separated even before the A_{2A} receptors emerged [54]. The A_{2A} receptor possesses an asparagine residue adjacent to the cysteine residue corresponding to C154, but the sequon is lost, probably in favor for gaining more stability of the loops through disulfide bonds. Curiously, the mutant C154S showed an 8-fold decrease in affinity for the antagonist PSB-603, while agonist binding was not significantly altered as compared to the wild-type (Supplemental Figure 2, Table 2). Receptor function of the C154S mutant on the other hand was significantly altered depending on the agonist used. The nucleosidic agonist NECA was about three-fold less potent, while the non-nucleosidic agonist BAY60-6583 was slightly more potent at the C154S mutant receptor in comparison with the wild-type receptor.

This leads to the hypothesis that free cysteine residues, especially C154, could play a role in the interaction with specific ligands as it has been described for other GPCRs, e.g. for $P2Y_{12}$ [48], the β2 adrenergic receptor [55], or the cannabinoid receptor 2 [56]. Thus, free cysteine residues in the extracellular loops of the A_{2B} receptor may allow for the development of new drugs, especially for inhibiting receptor function.

A possible explanation for the occurrence of the high number of cysteine residues in the ECL2 of the A_{2B} receptor, which are not involved in disulfide bond formation under native conditions, could be that they are part of a regulatory system, which may, for

example, explain the down-regulation of A_{2B} receptors during oxidative stress. Such an effect has been described for alveolar macrophages from patients with chronic obstructive pulmonary disease [57]. Oxidative stress leads to more oxidizing conditions in the ER lumen, which in turn may lead to disulfide bond formation of non-native bonds, resulting in more misfolded proteins, more degradation and finally to less A_{2B} receptors at the cell surface. The A_{2A} receptor, which is upregulated under oxidative stress [45,57] would not be affected, because all four possible disulfide bonds are formed in the functional A_{2A} receptor, at least according to the X-ray structure [45], as well as according to a recent molecular modeling study [58].

The cysteine residues could be involved in controlling/regulating receptor function by forming so-called allosteric disulfide bonds, e.g. by promoting or stabilizing the active or inactive receptor conformation [54]. Since most X-ray structures of GPCRs reported to date represent the inactive, antagonist-bound conformation, it cannot be excluded that one or more cysteine residues might be involved in allosteric disulfide bonds and would either be reduced in the active receptor conformation or could have formed artificially during the crystallization process. Usually allosteric disulfide bonds are controlled by catalytic disulfides of oxidoreductases, which are regulated through changes in the oxidizing environment, e.g. through oxidative stress [54]. The fact that the structurally different ligands – PSB-603, NECA, and BAY60-6583 – resulted in different changes in IC_{50}- or EC_{50} (decreased or increased values) in the C154S mutant as compared to the wild-type receptor indicates that C154 may be directly or indirectly involved in ligand binding. However, this hypothesis cannot be confirmed by our homology model.

Free cysteine residues can also be involved in metal ion complexation, e.g. with Zn^{2+}, Pb^{2+} or Hg^{2+}. So far, reports about the role of metal ion complexation in the regulation of GPCRs are scarce. Inhibitory effects of Zn^{2+} on ligand binding at the serotonin receptor 5-HT_{1A} have been reported; the physiological significance, however, remained unclear [59]. A few other studies also showed allosteric effects of zinc ions on ligand binding at GPCRs (dopamine, metabotropic glutamate and β2-adrenergic receptors) with likewise unresolved physiological significance [60,61]. For several receptors, involvement of cysteine residues in dimerization has been shown. In these cases, however, cysteine residues were exclusively localized in the transmembrane domains or in intracellular loops [62,63].

In summary, we showed that the conserved disulfide bond between C3.25 in TMD3 and C45.50 in ECL2 is essential for adenosine A_{2B} receptor ligand binding and function and it also appears to improve transport of the receptors to the plasma membrane. Furthermore we have strong evidence that all other cysteine residues in the ECL2 are not involved in disulfide bond formation and if they were, that those bonds would not have any effects, neither on ligand binding, nor on receptor function. Only Cys154 appears to have small, significant effects on ligand binding. Thus, the cysteine residues in the ECL2 of the A_{2B} receptor may serve very different roles from those of the extracellular cysteine residues in the A_{2A} receptor.

Acknowledgements

A.C.S., D.T., and C.E.M. are supported by the state of NRW (NRW International Research Graduate School BIOTECH-PHARMA). T.B. was supported by a stipend provided by the Bischöfliche Studienförderung Cusanuswerk. We would like to thank Susan Jean Johns for upgrading the TOPO2 program to fulfill our needs for more colors in the topology model. We are also grateful to Dr. Thomas Krahn, Bayer Healthcare (Germany) for providing BAY60-6583.

Appendix A. Supplementary data

Supplementary data associated with this article can be found, in the online version, at doi:10.1016/j.bcp.2011.05.008.

References

[1] Burnstock G. Purine and pyrimidine receptors. Cell Mol Life Sci 2007;64:1471–83.
[2] Brunschweiger A, Müller CE. P2 receptors activated by uracil nucleotides—an update. Curr Med Chem 2006;13:289–312.
[3] Fredholm BB, IJzerman AP, Jacobson KA, Linden J, Müller CE. Nomenclature and classification of adenosine receptors – an update. Pharmacol Rev 2011;63:1–34.
[4] Schulte G, Fredholm BB. Signalling from adenosine receptors to mitogen-activated protein kinases. Cell Signal 2003;15:813–27.
[5] Linden J, Thai T, Figler H, Jin X, Robeva AS. Characterization of human A(2B) adenosine receptors: radioligand binding, western blotting, and coupling to G(q) in human embryonic kidney 293 cells and HMC-1 mast cells. Mol Pharmacol 1999;56:705–13.
[6] Feoktistov I, Biaggioni I. Adenosine A2B receptors. Pharmacol Rev 1997;49:381–402.
[7] Mirabet M, Mallol J, Lluis C, Franco R. Calcium mobilization in Jurkat cells via A_{2b} adenosine receptors. Br J Pharmacol 1997;122:1075–82.
[8] Pearson G, Robinson F, Beers Gibson T, Xu BE, Karandikar M, Berman K, et al. Mitogen-activated protein (MAP) kinase pathways: regulation and physiological functions. Endocr Rev 2001;22:153–83.
[9] Donoso MV, Lopez R, Miranda R, Briones R, Huidobro-Toro JP. A_{2B} adenosine receptor mediates human chorionic vasoconstriction and signals through arachidonic acid cascade. Am J Physiol Heart Circ Physiol 2005;288:H2439–4.
[10] Müller CE, Jacobson KA. Recent developments in adenosine receptor ligands and their potential as novel drugs. Biochim Biophys Acta 2010;1808:1290–308.
[11] Borrmann T, Hinz S, Bertarelli DC, Li W, Florin NC, Scheiff AB, et al. 1-Alkyl-8-(piperazine-1-sulfonyl)phenylxanthines: development and characterization of adenosine A_{2B} receptor antagonists and a new radioligand with subnanomolar affinity and subtype specificity. J Med Chem 2009;52:3994–4006.
[12] Yan L, Burbiel JC, Maass A, Müller CE. Adenosine receptor agonists: from basic medicinal chemistry to clinical development. Expert Opin Emerg Drugs 2003;8:537–76.
[13] Baraldi PG, Tabrizi MA, Fruttarolo F, Romagnoli R, Preti D. Recent improvements in the development of A(2B) adenosine receptor agonists. Purinergic Signal 2008;4:287–303 [Epub 2008, April 29].
[14] Fredholm BB. Adenosine, an endogenous distress signal, modulates tissue damage and repair. Cell Death Differ 2007;14:1315–23.
[15] Kong T, Westerman KA, Faigle M, Eltzschig HK, Colgan SP. HIF-dependent induction of adenosine A_{2B} receptor in hypoxia. FASEB J 2006;20:2242–50.
[16] Beukers MW, van Oppenraaij J, van der Hoorn PP, Blad CC, den Dulk H, Brouwer J, et al. Random mutagenesis of the human adenosine A_{2B} receptor followed by growth selection in yeast. Identification of constitutively active and gain of function mutations. Mol Pharmacol 2004;65:702–10.
[17] Ryzhov S, Zaynagetdinov R, Goldstein AE, Novitskiy SV, Dikov MM, Blackburn MR, et al. Effect of A2B adenosine receptor gene ablation on proinflammatory adenosine signaling in mast cells. J Immunol 2008;180:7212–20.
[18] Trincavelli ML, Marroni M, Tuscano D, Ceruti S, Mazzola A, Mitro N, et al. Regulation of A2B adenosine receptor functioning by tumour necrosis factor a in human astroglial cells. J Neurochem 2004;91:1180–90.
[19] Ryzhov S, Novitskiy SV, Zaynagetdinov R, Goldstein AE, Carbone DP, Biaggioni I, et al. Host A(2B) adenosine receptors promote carcinoma growth. Neoplasia 2008;10:987–95.
[20] Volpini R, Costanzi S, Vittori S, Cristalli G, Klotz KN. Medicinal chemistry and pharmacology of A2B adenosine receptors. Curr Top Med Chem 2003;3:427–43.
[21] Pastorin G, Federico S, Paoletta S, Corradino M, Cateni F, Cacciari B, et al. Synthesis and pharmacological characterization of a new series of 5,7-disubstituted-[1,2,4]triazolo[1,5-a][1,3,5]triazine derivatives as adenosine receptor antagonists: a preliminary inspection of ligand-receptor recognition process. Bioorg Med Chem 2010;18:2524–36.
[22] Pastorin G, Da Ros T, Spalluto G, Deflorian F, Moro S, Cacciari B, et al. Pyrazolo[4,3-e]-1,2,4-triazolo[1,5-c]pyrimidine derivatives as adenosine receptor antagonists. Influence of the N5 substituent on the affinity at the human A 3 and A 2B adenosine receptor subtypes: a molecular modeling investigation. J Med Chem 2003;46:4287–96.
[23] Beukers MW, den Dulk H, van Tilburg EW, Brouwer J, IJzerman AP. Why are A(2B) receptors low-affinity adenosine receptors? Mutation of Asn273 to Tyr increases affinity of human A(2B) receptor for 2-(1-Hexynyl)adenosine. Mol Pharmacol 2000;58:1349–56.
[24] Matharu AL, Mundell SJ, Benovic JL, Kelly E. Rapid agonist-induced desensitization and internalization of the A(2B) adenosine receptor is mediated by a serine residue close to the COOH terminus. J Biol Chem 2001;276:30199–207.
[25] Peeters MC, van Westen GJ, Guo D, Wisse LE, Müller CE, Beukers MW, et al. GPCR structure and activation: an essential role for the first extracellular loop in activating the adenosine A_{2B} receptor. FASEB J 2010;4:4.

[26] Ivanov AA, Palyulin VA, Zefirov NS. Computer aided comparative analysis of the binding modes of the adenosine receptor agonists for all known subtypes of adenosine receptors. J Mol Graph Model 2007;25:740–54.
[27] Ivanov AA, Baskin II, Palyulin VA, Piccagli L, Baraldi PG, Zefirov NS. Molecular modeling and molecular dynamics simulation of the human A_{2B} adenosine receptor. The study of the possible binding modes of the A_{2B} receptor antagonists. J Med Chem 2005;48:6813–20.
[28] Kim YC, de Zwart M, Chang L, Moro S, von Frijtag Drabbe Kunzel JK, Melman N, et al. Derivatives of the triazoloquinazoline adenosine antagonist (CGS 15943) having high potency at the human A_{2B} and A_3 receptor subtypes. J Med Chem 1998;41:2835–45.
[29] Sherbiny FF, Schiedel AC, Maass A, Müller CE. Homology modelling of the human adenosine A2B receptor based on X-ray structures of bovine rhodopsin, the beta2-adrenergic receptor and the human adenosine A_{2A} receptor. J Comput Aided Mol Des 2009;23:807–28.
[30] Ballesteros J, Weinstein H. Integrated methods for the constructionof three-dimensional models of structure-function relations in G protein-coupled receptors. Meth Neurosci 1995;25:366–428.
[31] de Graaf C, Foata N, Engkvist O, Rognan D. Molecular modeling of the second extracellular loop of G-protein coupled receptors and its implication on structure-based virtual screening. Proteins 2008;71:599–620.
[32] Avlani VA, Gregory KJ, Morton CJ, Parker MW, Sexton PM, Christopoulos A. Critical role for the second extracellular loop in the binding of both orthosteric and allosteric G protein-coupled receptor ligands. J Biol Chem 2007;282:25677–86.
[33] http://www.ebi.ac.uk/Tools/clustalw2/ (27.01.2011).
[34] http://www.ebi.ac.uk/Tools/emboss/align/ (27.01.2011).
[35] http://www.cbs.dtu.dk/services/NetNGlyc/ (27.01.2011).
[36] http://www.sacs.ucsf.edu/TOPO2/ (27.01.2011).
[37] http://modbase.compbio.ucsf.edu/modloop/ (27.01.2011).
[38] http://ambermd.org/ (27.01.2011).
[39] http://www.ebi.ac.uk/thornton-srv/software/PROCHECK/ (27.01.2011).
[40] Sippl MJ. Recognition of errors in three-dimensional structures of proteins. Proteins 1993;17:355–62.
[41] Lowry OH, Rosebrough NJ, Farr AL, Randall RJ. Protein measurement with the Folin phenol reagent. J Biol Chem 1951;193:265–75.
[42] Hillmann P, Ko GY, Spinrath A, Raulf A, von Kügelgen I, Wolff SC, et al. Key determinants of nucleotide-activated G protein-coupled P2Y(2) receptor function revealed by chemical and pharmacological experiments, mutagenesis and homology modeling. J Med Chem 2009;52:2762–75.
[43] Motulsky HJ, Christopoulos A. Fitting models to biological data using linear and nonlinear regression. San Diego: GraphPad Software Inc; 2003.
[44] Nordstedt C, Fredholm BB. A modification of a protein-binding method for rapid quantification of cAMP in cell-culture supernatants and body fluid. Anal Biochem 1990;189:231–4.
[45] Jaakola VP, Griffith MT, Hanson MA, Cherezov V, Chien EY, Lane JR, et al. The 2.6 angstrom crystal structure of a human A_{2A} adenosine receptor bound to an antagonist. Science 2008;322:1211–7.
[46] Peeters MC, van Westen GJ, Li Q, IJzerman AP. Importance of the extracellular loops in G protein-coupled receptors for ligand recognition and receptor activation. Trends Pharmacol Sci 2011;32:35–42.
[47] Karnik SS, Sakmar TP, Chen HB, Khorana HG. Cysteine residues 110 and 187 are essential for the formation of correct structure in bovine rhodopsin. Proc Natl Acad Sci U S A 1988;85:8459–63.
[48] Ding Z, Kim S, Dorsam RT, Jin J, Kunapuli SP. Inactivation of the human $P2Y_{12}$ receptor by thiol reagents requires interaction with both extracellular cysteine residues, Cys17 and Cys270. Blood 2003;101:3908–14.
[49] Shi L, Javitch JA. The second extracellular loop of the dopamine D2 receptor lines the binding-site crevice. Proc Natl Acad Sci U S A 2004;101:440–5.
[50] Duong HT, Gao ZG, Jacobson KA. Nucleoside modification and concerted mutagenesis of the human A_3 adenosine receptor to probe interactions between the 2-position of adenosine analogs and Gln167 in the second extracellular loop. Nucleosides Nucleotides Nucleic Acids 2005;24:1507–17.
[51] Bokoch MP, Zou Y, Rasmussen SG, Liu CW, Nygaard R, Rosenbaum DM, et al. Ligand-specific regulation of the extracellular surface of a G-protein-coupled receptor. Nature 2010;463:108–12.
[52] Ai LS, Liao F. Mutating the four extracellular cysteines in the chemokine receptor CCR6 reveals their differing roles in receptor trafficking, ligand binding, and signaling. Biochemistry 2002;41:8332–41.
[53] McGinnes LW, Morrison TG. Disulfide bond formation is a determinant of glycosylation site usage in the hemagglutinin-neuraminidase glycoprotein of Newcastle disease virus. J Virol 1997;71:3083–9.
[54] Azimi I, Wong JW, Hogg PJ. Control of mature protein function by allosteric disulfide bonds. Antioxid Redox Signal 2011;14:113–26.
[55] Rubenstein LA, Zauhar RJ, Lanzara RG. Molecular dynamics of a biophysical model for beta2-adrenergic and G protein-coupled receptor activation. J Mol Graph Model 2006;25:396–409.
[56] Mercier RW, Pei Y, Pandarinathan L, Janero DR, Zhang J, Makriyannis A. hCB2 ligand-interaction landscape: cysteine residues critical to biarylpyrazole antagonist binding motif and receptor modulation. Chem Biol 2010;17:1132–42.
[57] Varani K, Caramori G, Vincenzi F, Tosi A, Barczyk A, Contoli M, et al. Oxidative/nitrosative stress selectively altered A2B adenosine receptors in chronic obstructive pulmonary disease. FASEB J 2009;14:14.
[58] Goddard 3rd WA, Kim SK, Li Y, Trzaskowski B, Griffith AR, Abrol R. Predicted 3D structures for adenosine receptors bound to ligands: comparison to the crystal structure. J Struct Biol 2010;170:10–20.
[59] Barrondo S, Salles J. Allosteric modulation of 5-HT(1A) receptors by zinc: binding studies. Neuropharmacology 2009;56:455–62 [Epub 2008, October 14].
[60] Schetz JA, Chu A, Sibley DR. Zinc modulates antagonist interactions with D2-like dopamine receptors through distinct molecular mechanisms. J Pharmacol Exp Ther 1999;289:956–64.
[61] Elling CE, Frimurer TM, Gerlach LO, Jorgensen R, Holst B, Schwartz TW. Metal ion site engineering indicates a global toggle switch model for seven-transmembrane receptor activation. J Biol Chem 2006;281:17337–46 [Epub 2006, March 27].
[62] Klco JM, Lassere TB, Baranski TJ. C5a receptor oligomerization. I. Disulfide trapping reveals oligomers and potential contact surfaces in a G protein-coupled receptor. J Biol Chem 2003;278:35345–53.
[63] Berthouze M, Rivail L, Lucas A, Ayoub MA, Russo O, Sicsic S, et al. Two transmembrane Cys residues are involved in 5-HT4 receptor dimerization. Biochem Biophys Res Commun 2007;356:642–7.